SAR China Land Mapping Project: Development, Production and Potential Applications

SAR China Land Mapping Project: Development, Production and Potential Applications

Lu Zhang[1], **Huadong Guo, Guang Liu, Wenxue Fu, Shiyong Yan, Rui Song, Peng Ji, Xinyuan Wang**
[1] Key Laboratory of Digital Earth Science, Institute of Remote Sensing and Digital Earth, Chinese Academy of Sciences

E-mail: luzhang@ceode.ac.cn

Abstract: Large-area, seamless synthetic aperture radar (SAR) mosaics can reflect overall environmental conditions and highlight general trends in observed areas from a macroscopic standpoint, and effectively support research at the global scale, which is in high demand now across scientific fields. The SAR China Land Mapping Project (SCLM), supported by the Digital Earth Science Platform Project initiated and managed by the Center for Earth Observation and Digital Earth, Chinese Academy of Sciences (CEODE), is introduced in this paper. This project produced a large-area SAR mosaic dataset and generated the first complete seamless SAR map covering the entire land area of China using EnviSat-ASAR images. The value of the mosaic map is demonstrated by some potential applications in studies of urban distribution, rivers and lakes, geologic structures, geomorphology and paleoenvironmental change.
Keywords: Synthetic aperture radar (SAR), EnviSat-ASAR, large area mosaic, China

1. Introduction

Synthetic aperture radar (SAR), an active microwave sensor, has become internationally recognized as an important, cutting-edge technology for Earth observation. With all-weather, day-night imaging and partial penetrating capability, SAR has become a sophisticated tool for global change detection [1] [2] [3], resource exploration [4] disaster assessment [5], urban [6] environment monitoring) and studies of other planets [7].

Recently, SAR applications have been focusing more and more on solving the important scientific problems of the global environment monitoring [8]. Therefore, large-area Earth observation studies are gaining more and more attention. One advantage is that large-area, seamless SAR mosaic maps have the capability to reflect the overall environmental conditions of the observed area, therefore providing a macroscopic standpoint to analyze general trends. At the same time, these SAR mosaic maps are also base data for the development of Digital Earth, a new, advanced concept for observing, analyzing, and researching the Earth [9] [10].

Many large-area mapping projects based on SAR data have been conducted and provided abundant, valuable datasets for many research fields. Through collaboration between the National Aeronautics and Space Administration (NASA) and the Canadian Space Agency (CSA), the

Corresponding author: Lu Zhang, luzhang@ceode.ac.cn.

RADARSAT-1 Antarctic Mapping Project (RAMP) was developed to map Antarctica using RADARSAT-1 SAR data. The project proceeded in two parts. The first was called Antarctic Mapping Mission-1 and acquired data in 1997, resulting in the first high-resolution (25 m) radar map of Antarctica. The second part, called the Modified Antarctic Mapping Mission (MAMM), which took place in 2000, exploited interferometric repeat-pass observations to estimate glacier surface velocities [11]. The Global Rain Forest Mapping Project (GRFM) is an international collaborative effort initiated and managed by the National Space Development Agency of Japan (NASDA). The main goal of the project is to produce a high resolution, seamless mosaic map of the entire tropical rain forest domain in Africa, South America, Central America and other regions using L-band SAR data acquired from 1996 to 1997 from the JERS-1 spacecraft [12] [13]. Utilizing ERS-1 SAR data acquired in summer from 1992-1993, a nearly seamless, large-scale, terrain-corrected digital SAR mosaic of the state of Alaska was successfully generated at a pixel resolution of 100 m. The developed SAR dataset was applied in mapping soil moisture, forests, glaciers, and geologic and volcanic features [14]. Guo et al [15] generated a SAR mosaic of eastern China by using RADARSAT-1 data acquired in 1997. It was used to research the pattern of urban spatial structure in the Huanghuaihai Plain [16]. Using ERS-1/2 SAR data, the Chinese Academy of Forestry developed an interferometric SAR mosaic for generating a forest map [17]. In the last few years, global mosaics have been generated for the L-band using Advanced Land Observing Satellite (ALOS) phased array type L-band synthetic aperture radar (PALSAR) data [18] and for the X-band using TerraSAR-X radar data [19]. However, the datasets in China provide only incomplete coverage.

Using the aforementioned large-area SAR mosaic datasets, many research results have been produced that reflect the important value of these SAR mosaic products. This paper will introduce the SAR China Land Mapping project (SCLM), which is a sub-project of the Digital Earth Science Platform Project initiated and managed by the Center for Earth Observation and Digital Earth, Chinese Academy of Sciences (CEODE, CAS). The purpose of this project is to produce a large-area SAR mosaic of China with a resolution of 150 meters and generate the first complete and seamless SAR map covering the entire land area of China. The SAR data used in this project were acquired from the EnviSat-ASAR sensor in wide swath mode. The dataset produced in this project could provide conventional data support for analyzing the characteristics of SAR imagery of China from a macroscopic perspective covering many applications. It is also a necessary SAR data layer for the development of Digital China [2].

The processing and products of this SCLM project are introduced in Section 2. Examples of potential applications are described in Section 3, including research on urban distribution, rivers and lakes, geologic structures, and paleoenvironmental change in arid and semi-arid regions.

2. SAR China Land Mapping Project

2.1. Collection of SAR data

The land area of China is about 9.6 million square kilometers. Generation of a large-area, seamless SAR mosaic dataset and map that cover the entire land area of China requires abundant SAR data. Considering the quantity and resolution of SAR data, and the requirements for the study of SAR macroscopic characteristics of China, EnviSat-ASAR data in wide swath mode were used in this project. The swath width of the collected SAR is about 400 km. The pixel spacing and resolution of the SAR data are 75 m and 150 m, respectively. The acquisition time is from 2004 to 2005. The detailed parameters of the collected SAR data are shown in Table 1.

Table 1. Parameters of collected SAR data

Parameter	Value
Sensor	ASAR
Mode	Wide Swath
Resolution	150 m
Pixel spacing	75 m
Swath width	400 km
Acquisition time	2004-2005

2.2. Processing of SAR data

The SAR image processing used in this project included image preprocessing, terrain correction, image mosaic generation, and product generation.

2.2.1. Preprocessing

The collected SAR data needed to be preprocessed for latter processing such as absolute radiometric calibration, slant-to-ground range, SAR data filtering, and others.

The backscattering coefficients could be obtained from SAR data by using an absolute radiometric calibration method, which can provide better information for image interpretation. Since the mode of the collected SAR data is wide swath mode (ASA_WSM-1P), the absolute radiometric calibration formula expression is as follows [20],

$$\delta^0_{i,j} = \frac{DN^2_{i,j}}{K}\sin(\alpha_{i,j}) \tag{1}$$

Where δ^0 is the sigma nought or the backscattering coefficient, i is image line (i=1….L), j is image column ($j=1...M$), L and M are the number of image lines and columns; K is the absolute calibration constant; DN^2 is the pixel intensity value, and α is the incidence angle.

Speckle noise must be removed or weakened after the absolute calibration of SAR data because the speckle noise of SAR data is severe. The Lee filter method is chosen in this project because of its effectiveness in removing the speckle noise of SAR data [21].

2.2.2. Terrain correction

It is well known that SAR data have severe geometric and radiometric distortions over rugged terrain due to the nature of their peculiar, slant-range mapping [14] [22]. The larger the elevation is relative to the reference elevation, the more obvious the geometric distortion is. The result is foreshortening, layover and shadow effects for rugged terrain. The foreshortening effect compresses the backscattered signal energy coming from the foreshortened areas, i.e., the affected areas in the image appear brighter, and the shadow effect in radar imagery receives no information from the back slope.

Terrain correction includes geometric distortion correction and radiometric distortion correction, which can be removed by making use of the height information available within a digital elevation model (DEM). This project conducted the geometric distortion correction by matching the real SAR data with simulated SAR data derived from a DEM of China with 90 m resolution. The DEM data were obtained from the Shuttle Radar Topography Mission (SRTM). Apart from the geometric distortion correction, the radiometric distortion should be removed by using the local incidence angle obtained from DEM, instead of the incidence angle provided from the SAR orbit information [23]. The terrain correction used in this project has been applied successfully in many SAR mapping projects [3] [14].

Figure 1 is an example of the effect of terrain correction. The SAR data were acquired in Yunnan Province (the Hengduan Mountains are displayed in this figure). From the comparison between the slant-range SAR image (Figure 1a) and the terrain-corrected SAR image (Figure 1b), it is clear that the terrain-induced distortions, such as foreshortening and layover effects, have been removed effectively.

(a)slant-range SAR image (b)terrain-corrected SAR image

Figure 1. The effect of terrain correction of SAR data

2.2.3. Mosaic

After terrain correction, a mosaic of SAR data is needed for the generation of a large-area, seamless SAR image covering China. In this step, two problems are worthy of notice: (1) the terrain-corrected SAR data need to have precise and consistent geocoding, or misplacement of images will appear; (2) the balancing of the backscattering coefficient for the adjacent SAR data is required to avoid color differences in the mosaic due to the differences of acquisition time and incidence angles in the adjacent SAR data.

Because the SRTM 90-m DEM data used in this project exceed the terrain correction of SAR data with 150 meter resolution, the terrain-corrected SAR data have more precise geocoding. An energy normalization method is often used to reduce the difference of backscattering energy among the adjacent data [24]. In addition, when generating the SAR mosaic, the choices of seam lines and color-matching regions deserve close attention. The seam lines should be as far away as possible from the typical ground objects, such as towns, lakes and so on. Therefore, these targets were chosen from a single SAR image rather than multiple. To explain the processing of SAR data clearly, Figure 2 shows the entire process applied in this project to generate the SAR mosaic.

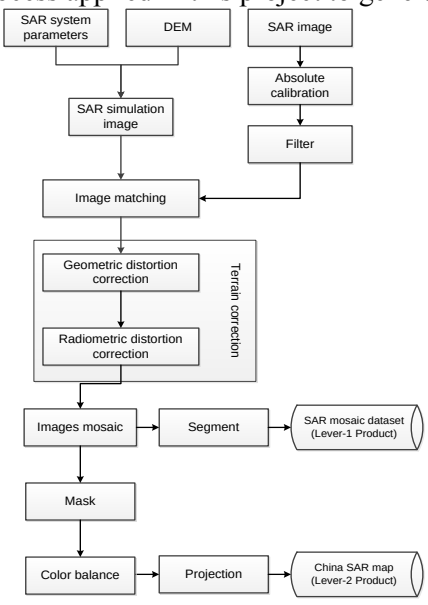

Figure 2. Process for generating the SAR mosaic map of China

2.2. Products

The SCLM project will produce two levels of products. One is the backscattering coefficient product of all land in China, which belongs to the Level-1 product. These data are stored in Geotiff files with a 32-bit floating-point data type. The geocoding system of this level of product is World Geodetic System 1984 (WGS-84). For the convenience of image processing and product transmission, the data are divided into 22 mapsheets according to longitude and latitude segmentation with a size of (10×10) degrees. The longitude of this product ranges from 70 degrees to 140 degrees, and the latitude ranges from 10 degrees to 60 degrees. The index map of the product is shown in Figure 3. Another product is the first seamless grey SAR map covering all land in China. The map is also stored as a Geotiff file with an 8-bit data type, which belongs to the Level-2 product. The projection of this map is Xi'an 80 (Figure 4).

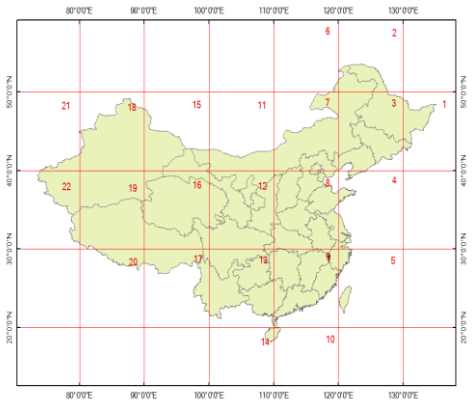

Figure 3. Index map of the SAR mosaic of China

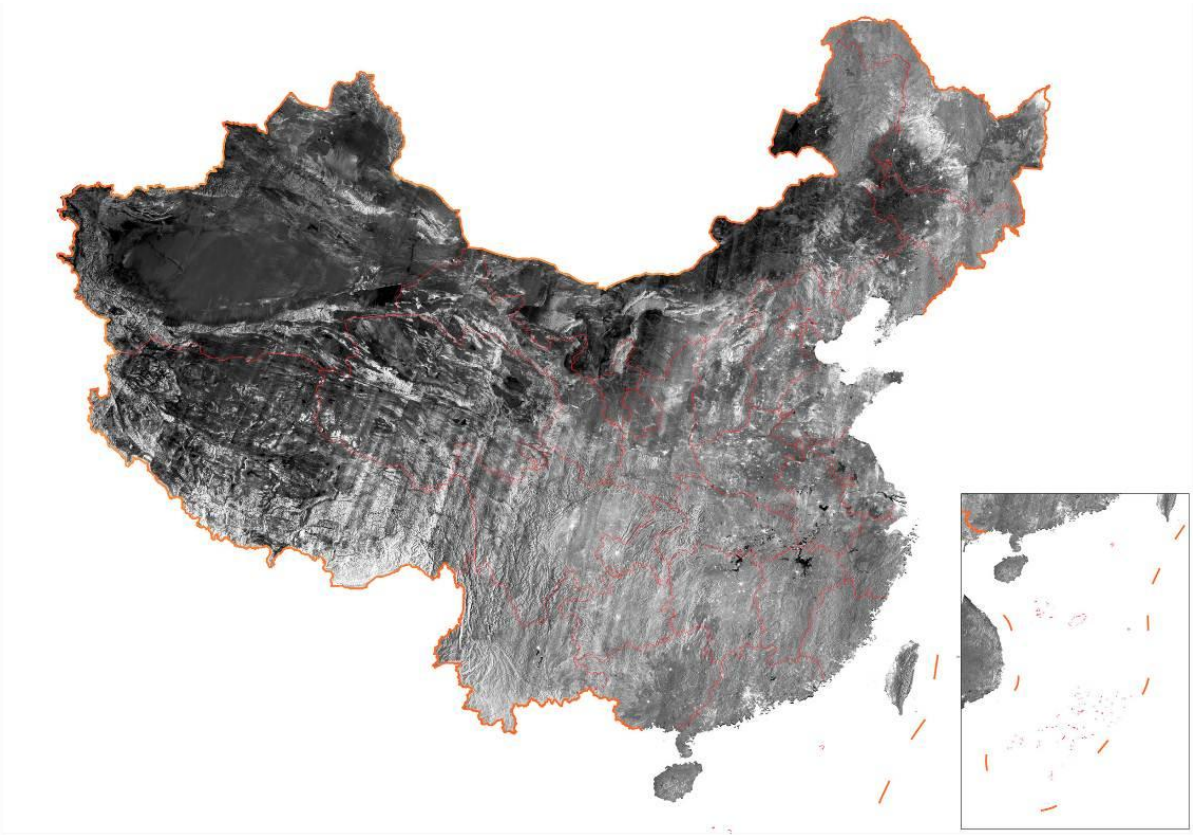

Figure 4. China SAR map (the projection is Xi'an 80)

3. Potential applications

3.1. Urban distribution

Because of the characteristics of geometry and materials, buildings in cities and towns often form dihedral structures and produce strong double-bounce scattering, therefore bringing about strong back echo returning to the side-looking SAR sensor. Urban regions are prominently displayed in SAR images as a bright area. As a result, SAR imagery is very suitable for urban research, including residential area detection, population estimation, land cover use, urban land use change and urbanization, urban social economic conditions analysis, impact of human activities on the environment and so on [22]. The large-area SAR mosaic dataset of China generated in this project can provide more valuable data for the study of urban distribution in China from a macroscopic perspective, not only because of the sensitivity of SAR images to buildings, but also its all-weather, day-night capabilities.

Based on the China SAR mosaic dataset, the urban position and scope can be clearly demonstrated and extracted. Combined with relevant information, the data can be used to study the characteristics of urban distribution in China, giving an understanding of the spatial structure and developing trends of Chinese urban systems. As an example, the SAR mosaic map of part of eastern China is shown in Figure 5. The cities and towns in this region are obvious, bright areas and the general features of the urban spatial distribution can quickly be determined. One is that the locations of most cities and towns are decided by the transportation network. The line of cities between Beijing, Shijiazhuang, Zhengzhou, and Wuhan shows the location of the Beijing-Guangzhou railway, which is one of the most important railways in China, throughout the north and south. Another is that at a wider scale, the cities here seem to be a mirror image when looking at the line of cities between Taiyuan, Zhengzhou and Wuhan as an axis of symmetry. These conclusions are consistent with the results conducted by Guan [25] and Chen [26], therefore showing the potential of the SAR mosaic for studies of urban spatial structure.

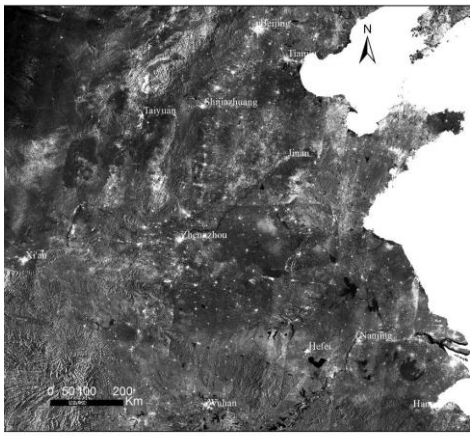

Figure 5. Urban distribution in eastern China shown in the SAR mosaic map

In addition, some densely-urbanized regions have formed along China's coast, such as the Pearl River Delta, the Yangtze River Delta and the Beijing-Tianjin-Hebei region. As examples, the SAR images of the Beijing-Tianjin-Hebei region and the Pearl River Delta from the China SAR mosaic map are shown in Figure 6(a) and (b), respectively. The cities and towns are concentrated and connected gradually, forming agglomerations (mega-cities), which will have a key role in China's future urban distribution, replacing individual cities. As a result, the SAR mosaic is also useful for studying the growth of urban agglomerations.

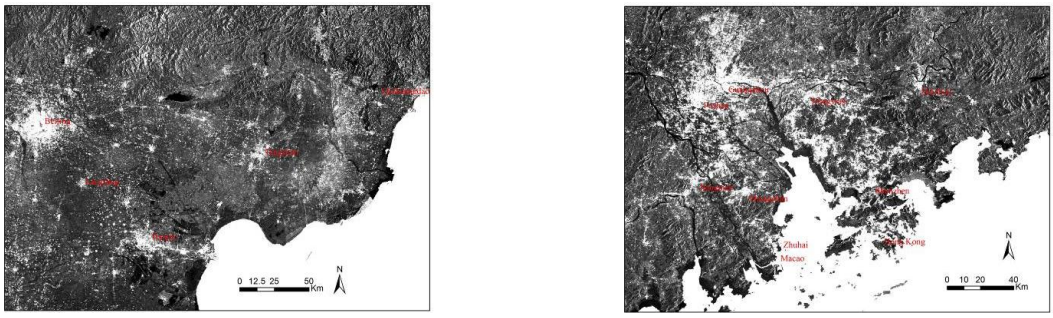

(a) Beijing-Tianjin-Hebei region (b) the Pearl River Delta

Figure 6. The SAR images of densely-urbanized regions

3.2. Rivers and lakes

Contrary to cities and towns, the backscattering echo of rivers and lakes is very weak, which are shown as obvious dark regions in SAR images [27]. One of the reasons is the smooth water surface relative to the sea surface, which effectively causes the specular reflection. Another reason is the high dielectric constant, which gives rise to the strong absorption of electromagnetic wave power. As a result, SAR images have a strong detection capability for inland water bodies.

Figure 7 shows a SAR mosaic of the middle and lower Yangtze River. Hundreds of lakes and tributaries of different sizes along the Yangtze River are displayed clearly, including some larger lakes, such as Dongting Lake, Poyang Lake, Cao Lake and Tai Lake. The large-area SAR mosaic data generated in this project can be effectively applied to conduct watershed-scale research on rivers and lakes. The research fields include the distribution of water bodies, change of water surface area, and flood detection, and so on [15].

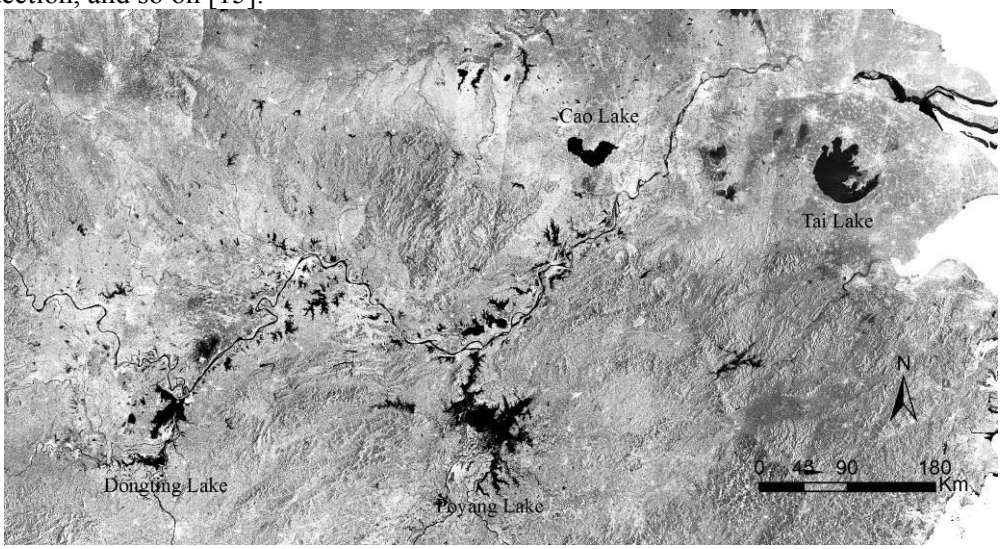

Figure 7. SAR mosaic of the middle and lower Yangtze River

3.2. Geologic structure

SAR data have been proved to be sensitive to linear structures [22]. This, together with the ability to partially penetrate vegetation, clouds, rain and arid surfaces, makes SAR one of the most effective sensors for the analysis of geologic structure and morphology. In addition, the side-looking observation approach of SAR sensors can produce images with strong stereo perception. Two examples obtained from the SAR mosaic of China are demonstrated in Figure 8 and Figure 9. One is

the comb folds in eastern Sichuan Province; another is the Altun Tagh fault, one of the famous Northwest-East sinistral strike-slip faults in northwestern China.

Figure 8 shows the eastern region of the Sichuan basin, where Daba Mountain in the north and the comb folds in the east are located. The orientation and distribution of the folds in this SAR image are obvious. They can be identified as the trough-like and ejective folds typical in China [28]. Figure 9 is the SAR image of the northwestern region of China. Several large linear structures can be discovered, as noted by the arrows, which indicate the Altun Tagh fault in northwestern China. As a result, it can be concluded that the SAR mosaics have the potential to provide data support for large-area geological studies, especially in regions where field surveys are difficult.

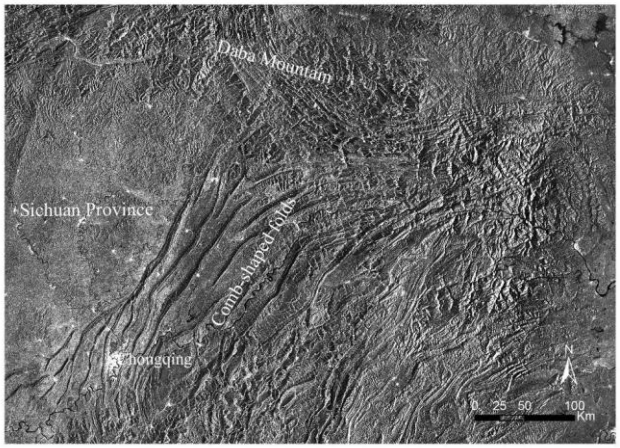

Figure 8. SAR image of Daba Mountain and comb-shaped folds

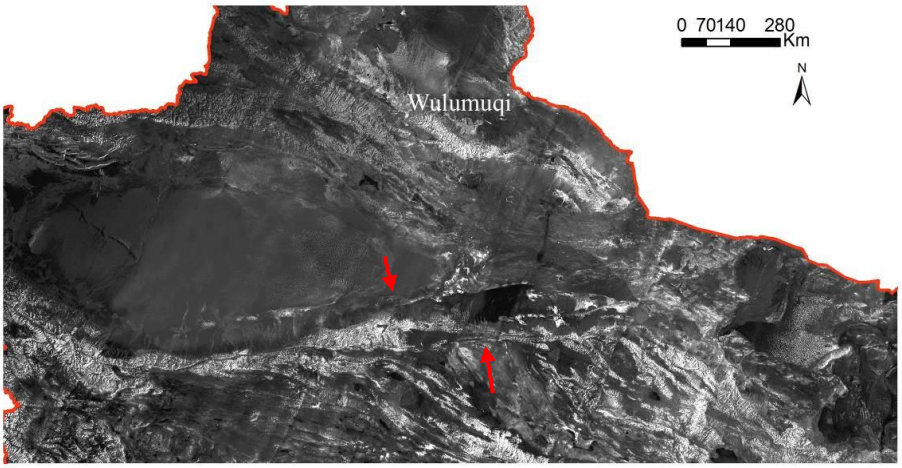

Figure 9. SAR image of Altun Tagh fault in northwestern China

3.3. Environmental changes of arid and semi-arid regions

Apart from the sensitivity of geologic structures and lithology, SAR images have the capability to effectively detect topography and geomorphology due to SAR's sensitivity to the characteristics of the ground surface, especially in areas with adverse natural environments, such as canyons, alluvial fans, sand dunes, loess, and karst landforms. Also, the penetrative characteristic of SAR enables SAR images to clearly display ancient water systems under dry, sandy surfaces [29], therefore providing more useful information supporting the analysis of paleogeomorphology and environmental evolution in arid and semi-arid regions.

As a typical example, the SAR mosaic of the Alashan Plateau in northern China is shown in Figure 10. Ejin alluvial fan, one of the largest alluvial fans in the world, is located in the west of this area, while three deserts formed from ancient lake basins are located in the east, i.e., Badain Jaran

Desert, Tenggeli Desert, and Wulanbuhe Desert. From this figure, the distribution of alluvial fan units with different ages can be identified by utilizing the characteristics of the ground surface obtained from the SAR image [30]. In addition, some water systems are obvious in this figure, such as ancient rivers and lakes [31], due to the penetrative capability of SAR. The area marked by "A" in the Ejin alluvial fan and the "sand rivers" marked by "B" are the courses of shifting sand formed by ancient river valleys. As a result, the example reflects the potential of the SAR mosaic to aid in the study of topography, geomorphology, ancient water systems, and paleoenvironmental evolution.

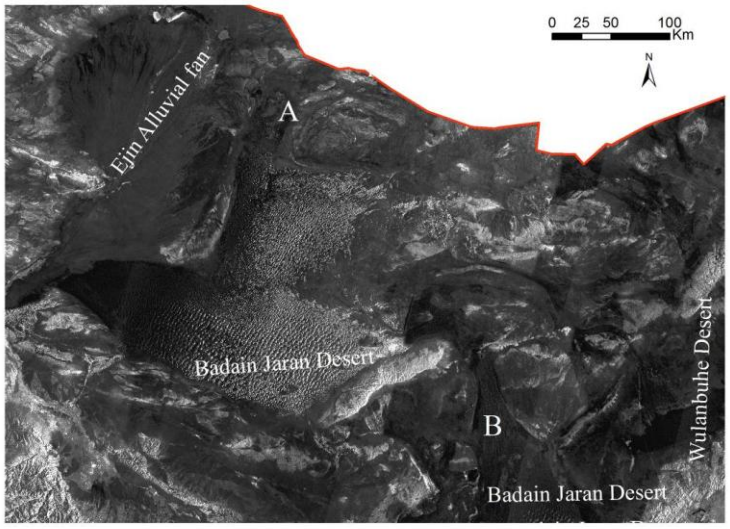

Figure 10. SAR mosaic of the Alashan Plateau in northern China

4. Conclusions

The SAR China Land Mapping project, supported by the Digital Earth Science Platform Project initiated and managed by CEODE, is introduced in this paper. This project produced a large-area SAR mosaic dataset and the first complete, seamless SAR map covering all of China from EnviSat-ASAR images with a resolution of 150 meters. The SAR image processing used in this project included image preprocessing, terrain correction, image mosaic generation, masking and color balance. Two levels of products were generated, including backscattering coefficient data for all of China with 32-bit floating-point data (Level 1, WGS-84), and a seamless SAR grey map of China with an 8-bit data type and Xi'an '80 projection (Level 2). The dataset produced in this project can provide conventional data support to analyze the characteristics of SAR images of China from a macroscopic perspective covering many applications.

Based on the support of this product, some potential applications were discussed, such as urban distribution in eastern China, rivers and lakes around the middle and lower Yangtze River, the comb folds in eastern Sichuan Province, the large Altun Tagh fault in northwestern China, and paleoenvironmental change research in the Alashan Plateau. These examples reflect the value of the SAR mosaic of China in many applications, including detection of global change, resource exploration, geologic surveying, and urban environment monitoring.

Acknowledgements

This research is supported by Natural Science Foundation of China (NO. 41001268), and Digital Earth Science Platform Project initiated and managed by the Center for Earth Observation and Digital Earth, Chinese Academy of Sciences (CEODE).

References

[1] Stofan E R, Evans D L, Schmullius C, Holt B, Plaut J J, Van Zyl J, Wall S D and Way J 1995 Overview of results of spaceborne imaging radar-c, x-band synthetic aperture radar (sir-c/x-SAR) *IEEE Trans. Geosci. Remote. Sensing* **33(4)** 817-828

[2] Shupeng C and van Genderen J 2008 Digital Earth in support of global change research *International Journal of Digital Earth* **1(1)** 43-65

[3] Shimada M and Ohtaki T 2010 Generating Large-Scale High-Quality SAR Mosaic Datasets: Application to PALSAR Data for Global Monitoring *IEEE Journal of selected topics in applied earth observations and remote sensing* **3(4)** 637-656

[4] Dabbagh A E, AlHinai K G and Khan M A 1997 Detection of sand-covered geologic features in the arabian peninsula using sir-c/x-sar data *Remote Sensing of Environment*. **59(2)** 375-382

[5] Guo H D, Wang X Y, Li X W, Liu G, Zhang L and Yan S Y 2010 Yushu earthquake synergic analysis using multimodal SAR datasets *Chinese Science Bulletin.* **55(31)** 3499-3503

[6] Lee J S, Ainsworth T L, Kelly J P and Lopez-Martinez C 2008 Evaluation and Bias Removal of Multilook Effect On Entropy/Alpha/Anisotropy in Polarimetric SAR Decomposition *IEEE Trans. Geosci. Remote. Sensing*. **46(10)** 3039-3052

[7] Paillou P Y, Lasne E, Heggy J M and Malezi éux 2006 A study of p-band synthetic aperture radar applicability and performance for mars exploration: imaging subsurface geology and detecting shallow moisture *Journal of Geophysical Research-Planets* 111(E6)

[8] Guo H D and Li X W 2011 Technical characteristics and potential application of the new generation SAR for earth observation (in chinese) *Chinese Science Bulletin* **15(56)** 1155-1168

[9] Goodchild M F 2008 The use cases of digital earth *International Journal of Digital Earth.* **1(1)** 31-42

[10] Guo H D, Liu Z and Zhu L W 2010 Digital Earth: decadal experiences and some thoughts *International journal of digital earth.* **3(1)** 31-46

[11] Jezek K C 2008 The radarsat-1 antarctic mapping project *Byrd Polar Research Center - Report* No. 22

[12] Rosenqvist A and Birkett C M 2002 Evaluation of jers-1 SAR mosaics for hydrological applications in the Congo River basin *International Journal of Remote Sensing* **23(7)** 1283-1302

[13] Rosenqvist, A., et al., Rosenqvist A, Shimada M, Chapman B, McDonald K, Grandi G D, Jonsson H, Williams C, Rauste Y, Nilsson M, Sango D and M. Matsumoto 2004 An overview of the jers-1 SAR global boreal forest mapping (gbfm) project *International Geoscience and Remote Sensing Symposium (IGARSS)* Anchorage, AK, United states: 1033-1036

[14] Li S S, Guritz R, Logan T, Shindle M, Groves J, Olmsted C and Carsey F 1999 Summer environmental mapping potential of a large-scale ers-1 SAR mosaic of the state of Alaska *International Journal of Remote Sensing.* **20(2)** 387-401

[15] Guo H D 2001 Radar remote sensing applications in china *New York, Taylor & Francis Inc*

[16] Wang X Y, Fan X T and Guo H D 2001 Pattern analysis of spatial structure of urban system dominated by physical geographic factors *Progress in Geography* **20(1)** 67-72

[17] Li Z Y, Pang Y, Schmullius C and Santoro M 2005 Forest mapping using ENVISAT and ERS SAR data in northeast of china *International Geoscience and Remote Sensing Symposium (IGARSS)* Seoul, Korea, Republic of: 5670-5673

[18] Shimada M, Tadono T and Rosenqvist A 2010 Advanced land observing satellite (ALOS) and monitoring global environmental change *Proceedings of the IEEE* **98(5)** 780-799

[19] Rizzoli P, Bra¨ utigam B, Wollstadt S and Mittermayer J 2011 Radar Backscatter Mapping Using TerraSAR-X *IEEE Trans. Geosci. Remote. Sensing.* **49(10)** 3538-3547

[20] Rosich B and Meadows P 2004 Absolute calibration of ASAR lever 1 products generated with PF-ASAR *European Space Agency*

[21] Lee J S 1980 Digital image-enhancement and noise filtering by use of local statistics *IEEE Transactions on Pattern Analysis and Machine Intelligence.* **2(2)** 165-168

[22] Guo H D 2000 Radar earth observation theory and applications *Beijing, Science Press*

[23] Kellndorfer J M, Pierce L E, Dobson M C and Ulaby F T 1998 Toward consistent regional-to-global-scale vegetation characterization using orbital sar systems *IEEE Trans. Geosci. Remote. Sensing.* **36(5)** 1396-1411
[24] Dai X L and Khorram S 1998 The effects of image misregistration on the accuracy of remotely sensed change detection *IEEE Trans. Geosci. Remote. Sensing.* **36(5)** 1566-1577
[25] Guan C M and Cui G H 2004 Research on spatio-temporal distribution of chinese cities in the past over 100 years *Areal Research and Development.* **23(5)** 28-32
[26] Chen Y G and Yu B 2006 Bilateral symmetry of spatial distribution of cities in china *Advances in Earth Science*. **7** 687-694
[27] Shen G Z, Guo H D and Liao J J 2008 Object oriented method for detection of inundation extent using multi-polarized synthetic aperture radar image *J. Appl. Remote Sens.* **2(1)**
[28] Jiang B Q 1984 The mechanical mechanism of the trough-like and ejective folds in the east of sichuan province *Acta Geologica Sichuan* (0) 1-12
[29] McCauley J F, Schaber G G, Breed C S, Grolier M J, Haynes C V, Issawi B, Elachi C and R Blom 1982 Subsurface valleys and geoarcheology of the eastern Sahara revealed by shuttle radar *Science*. **218(4576)** 1004-1020
[30] Zhang L 2008 Research on characteristic extraction and object recognition based on full-polarization and multi-frequency imaging SAR --an case study of alluvial fans in china-Mongolian border area *Institute of Remote Sensing Applications, Chinese Academy of Sciences. Doctor*
[31] Guo H D, Liu H, Wang X Y, Shao Y and Sun Y 2000 Subsurface old drainage detection and paleoenvironment analysis using spaceborne radar images in alxa plateau *Science in China Series D-Earth Sciences.* **43(4)** 439-448